JOURNAL OF AIRCRAFT
Vol. 34, No. 6, November–December 1997

Maximization of the Fundamental Frequencies of Laminated Curved Panels Against Fiber Orientation

Hsuan-Teh Hu* and Chin-Deng Juang†
National Cheng Kung University, Tainan, Taiwan, Republic of China

The fundamental frequencies of fiber-reinforced laminated curved panels with a given material system are maximized with respect to fiber orientation by using a sequential linear programming method with a simple move-limit strategy. The significant influences of panel thickness, curvature, aspect ratio, cutouts, and end conditions on the maximum fundamental frequencies and the associated optimal fiber orientations are demonstrated.

Introduction

THE applications of fiber-composite laminate materials to primary components in advanced structures such as spacecraft, high-speed aircraft, and satellites have increased rapidly in recent years. Because many components of the aerospace structures are made of curved panels, a knowledge of dynamic characteristics of fiber-reinforced laminated panels, such as their fundamental frequencies, is essential.[1–3]

The fundamental frequencies of fiber-reinforced laminated curved panels depend highly on ply orientations, end conditions, and geometric variables such as panel curvature, thickness, aspect ratio, and cutouts.[4–12] Therefore, for composite panels with a given material system, geometric shape, thickness and end condition, the proper selection of appropriate lamination to maximize the fundamental frequency of the panels becomes a crucial problem.[13,14] However, in spite of the high potential for improved dynamic performance by use of composite optimization, there has not been much activity in this area.[15]

Research on the subject of structural optimization has been reported by many investigators.[16] Among various optimization schemes, the method of sequential linear programming has been successfully applied to many large-scale structural problems.[17,18] Hence, linearization of nonlinear optimization problems to meet requirements for iterative applications of a linear programming method is one of the most popular approaches to solve the structural optimization problem.

In this investigation, optimization of laminated curved panels to maximize their fundamental frequencies with respect to fiber orientations is performed by using a sequential linear programming method together with a simple move-limit strategy. The fundamental frequencies of laminated panels are calculated by using the ABAQUS finite element program.[19] In this paper, the constitutive equations for fiber-composite laminate, vibration analysis, and optimization method are briefly reviewed. Then the influence of end condition, panel curvature, thickness, aspect ratio, and cutouts on the optimal fundamental frequency and the associated optimal fiber orientation of composite panels is presented. Finally, important conclusions obtained from the study are given.

Received Dec. 10, 1995; presented as Paper 96-1585 at the AIAA/ASME/ASCE/AHS/ASC 37th Structures, Structural Dynamics and Materials Conference, Salt Lake City, UT, April 15–17, 1996; revision received Jan. 1, 1997; accepted for publication June 24, 1997.

*Associate Professor, Department of Civil Engineering. Senior Member AIAA.

†Research Assistant, Department of Civil Engineering.

Constitutive Matrix for Fiber-Composite Laminae

In the finite element analysis, the laminate panels are modeled by eight-node isoparametric laminate shell elements with six degrees of freedom per node (three displacements and three rotations). The formulation of the shell allows transverse shear deformation.[19,20] These shear flexible shells can be used for both thick- and thin-shell analyses.[19]

During the analysis, the constitutive matrices of composite materials at element integration points must be calculated before the stiffness matrices are assembled from element level to global level. For fiber-composite laminate materials, each lamina can be considered as an orthotropic layer in a plane stress condition (Fig. 1). The stress-strain relations for a lamina in the material coordinates (1,2,3) at an element integration point can be written as

$$\{\boldsymbol{\sigma}'\} = [Q_1']\{\boldsymbol{\varepsilon}'\} \tag{1}$$

$$\{\boldsymbol{\tau}'\} = [Q_2']\{\boldsymbol{\gamma}'\} \tag{2}$$

$$[Q_1'] = \begin{bmatrix} \dfrac{E_{11}}{1-\nu_{12}\nu_{21}} & \dfrac{\nu_{12}E_{22}}{1-\nu_{12}\nu_{21}} & 0 \\ \dfrac{\nu_{21}E_{11}}{1-\nu_{12}\nu_{21}} & \dfrac{E_{22}}{1-\nu_{12}\nu_{21}} & 0 \\ 0 & 0 & G_{12} \end{bmatrix} \tag{3}$$

$$[Q_2'] = \begin{bmatrix} \alpha_1 G_{13} & 0 \\ 0 & \alpha_2 G_{23} \end{bmatrix} \tag{4}$$

where $\{\boldsymbol{\sigma}'\} = \{\sigma_1, \sigma_2, \tau_{12}\}^T$, $\{\boldsymbol{\tau}'\} = \{\tau_{13}, \tau_{23}\}^T$, $\{\boldsymbol{\varepsilon}'\} = \{\varepsilon_1, \varepsilon_2, \gamma_{12}\}^T$, $\{\boldsymbol{\gamma}'\} = \{\gamma_{13}, \gamma_{23}\}^T$. The α_1 and α_2 are shear correction factors. In ABAQUS, the shear correction factors are calculated by assuming that the transverse shear energy through the thickness of laminate is equal to that of unidirectional bending.[19,21]

The constitutive equations for the lamina in the element coordinates (x, y, z) then become

$$\{\boldsymbol{\sigma}\} = [Q_1]\{\boldsymbol{\varepsilon}\}, \quad [Q_1] = [T_1]^T[Q_1'][T_1] \tag{5}$$

$$\{\boldsymbol{\tau}\} = [Q_2]\{\boldsymbol{\gamma}\}, \quad [Q_2] = [T_2]^T[Q_2'][T_2] \tag{6}$$

$$[T_1] = \begin{bmatrix} \cos^2\theta & \sin^2\theta & \sin\theta\cos\theta \\ \sin^2\theta & \cos^2\theta & -\sin\theta\cos\theta \\ -2\sin\theta\cos\theta & 2\sin\theta\cos\theta & \cos^2\theta - \sin^2\theta \end{bmatrix} \tag{7}$$

$$[T_2] = \begin{bmatrix} \cos\theta & \sin\theta \\ -\sin\theta & \cos\theta \end{bmatrix} \tag{8}$$

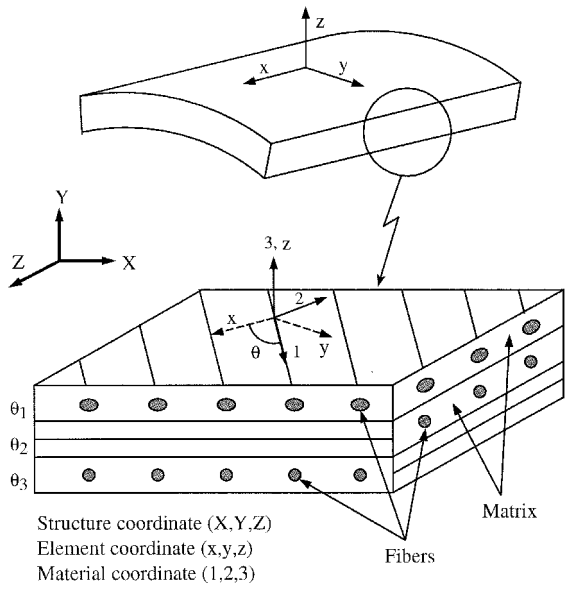

Fig. 1 Material, element, and structure coordinates of fiber-composite laminate curved panel.

where $\{\boldsymbol{\sigma}\} = \{\sigma_x, \sigma_y, \tau_{xy}\}^T$, $\{\boldsymbol{\tau}\} = \{\tau_{xz}, \tau_{yz}\}^T$, $\{\boldsymbol{\varepsilon}\} = \{\varepsilon_x, \varepsilon_y, \gamma_{xy}\}^T$, $\{\boldsymbol{\gamma}\} = \{\gamma_{xz}, \gamma_{yz}\}^T$, and θ is measured counterclockwise about the z axis from the element local x axis to the material 1 axis. The element coordinate (x, y, z) is a curvilinear local system (Fig. 1) that is different from the structural global coordinate (X, Y, Z). While the element x axis is parallel to the straight edge of the curved panel, element y and z directions are tangent and normal to the curved surface. Assume $\{\boldsymbol{\varepsilon}_0\} = \{\varepsilon_{x0}, \varepsilon_{y0}, \gamma_{xy0}\}^T$ are the in-plane strains at the midsurface of the laminate section and $\{\boldsymbol{\kappa}\} = \{\kappa_x, \kappa_y, \kappa_{xy}\}^T$ are the curvatures. The in-plane strains at a distance, z, from the midsurface become

$$\{\boldsymbol{\varepsilon}\} = \{\boldsymbol{\varepsilon}_0\} + z\{\boldsymbol{\kappa}\} \tag{9}$$

If h is the total thickness of the section, the stress resultants $\{\boldsymbol{N}\} = \{N_x, N_y, N_{xy}\}^T$, $\{\boldsymbol{M}\} = \{M_x, M_y, M_{xy}\}^T$, and $\{\boldsymbol{V}\} = \{V_x, V_y\}^T$ can be defined as

$$\{\boldsymbol{N}\} = \int_{-h/2}^{h/2} \{\boldsymbol{\sigma}\}\, dz = \int_{-h/2}^{h/2} [Q_1](\{\boldsymbol{\varepsilon}_0\} + z\{\boldsymbol{\kappa}\})\, dz \tag{10}$$

$$\{\boldsymbol{M}\} = \int_{-h/2}^{h/2} z\{\boldsymbol{\sigma}\}\, dz = \int_{-h/2}^{h/2} z[Q_1](\{\boldsymbol{\varepsilon}_0\} + z\{\boldsymbol{\kappa}\})\, dz \tag{11}$$

$$\{\boldsymbol{V}\} = \int_{-h/2}^{h/2} \{\boldsymbol{\tau}\}\, dz = \int_{-h/2}^{h/2} [Q_2]\{\boldsymbol{\gamma}\}\, dz \tag{12}$$

If there are n layers in the layup, Eqs. (10), (11), and (12) can be rewritten as a summation of integrals over the n laminae in the following forms:

$$\begin{Bmatrix} \{\boldsymbol{N}\} \\ \{\boldsymbol{M}\} \\ \{\boldsymbol{V}\} \end{Bmatrix} = \begin{bmatrix} (z_{jt} - z_{jb})[Q_1] & \frac{1}{2}(z_{jt}^2 - z_{jb}^2)[Q_1] & [0] \\ \frac{1}{2}(z_{jt}^2 - z_{jb}^2)[Q_1] & \frac{1}{3}(z_{jt}^3 - z_{jb}^3)[Q_1] & [0] \\ [0]^T & [0]^T & (z_{jt} - z_{jb})[Q_2] \end{bmatrix} \times \begin{Bmatrix} \{\boldsymbol{\varepsilon}_0\} \\ \{\boldsymbol{\kappa}\} \\ \{\boldsymbol{\gamma}\} \end{Bmatrix} \tag{13}$$

where z_{jt} and z_{jb} are the distance from the midsurface of the section to the top and the bottom of the jth layer, respectively. The [0] is a 3 by 2 matrix with all of the coefficients equal to zero. Note that for a laminate section with a symmetric layup, the extensional and the flexural terms in the constitutive matrix (13) become uncoupled, i.e.,

$$\sum_{j=1}^{n} \frac{1}{2}(z_{jt}^2 - z_{jb}^2)[Q_1] = \begin{bmatrix} 0 & 0 & 0 \\ 0 & 0 & 0 \\ 0 & 0 & 0 \end{bmatrix} \tag{14}$$

Vibration Analysis

For the finite element analysis of an undamped structure, if there are no external forces, the equation of motion of the structure can be written in the following form[22]:

$$[M]\{\ddot{\boldsymbol{D}}\} + [K]\{\boldsymbol{D}\} = \{\boldsymbol{0}\} \tag{15}$$

where $\{\boldsymbol{D}\}$ is a vector containing the unrestrained nodal degrees of freedom, $[M]$ is a structural mass matrix, $[K]$ a structural stiffness matrix, and $\{\boldsymbol{0}\}$ is a zero vector. Because $\{\boldsymbol{D}\}$ undergoes harmonic motion, the vectors $\{\boldsymbol{D}\}$ and $\{\ddot{\boldsymbol{D}}\}$ become

$$\{\boldsymbol{D}\} = \{\bar{\boldsymbol{D}}\}\sin \omega t, \qquad \{\ddot{\boldsymbol{D}}\} = -\omega^2\{\bar{\boldsymbol{D}}\}\sin \omega t \tag{16}$$

where the $\{\bar{\boldsymbol{D}}\}$ vector contains the amplitudes of the $\{\boldsymbol{D}\}$ vector and ω is the frequency. Equation (15) can then be written in an eigenvalue expression as

$$([K] - \lambda[M])\{\bar{\boldsymbol{D}}\} = \{\boldsymbol{0}\} \tag{17}$$

where $\lambda = \omega^2$ is the eigenvalue and $\{\bar{\boldsymbol{D}}\}$ becomes the eigenvector. In ABAQUS, a subspace iteration procedure[23] is used to solve for the eigenvalues, the natural frequency, and the eigenvectors. The obtained smallest natural frequency (fundamental frequency) is then the objective function for maximization.

Sequential Linear Programming

A general optimization problem may be defined as the following:
maximize

$$f(\underline{\boldsymbol{x}}) \tag{18a}$$

subjected to

$$g_i(\underline{\boldsymbol{x}}) \le 0, \qquad i = 1, \ldots, r \tag{18b}$$

$$h_j(\underline{\boldsymbol{x}}) = 0, \qquad j = r + 1, \ldots, m \tag{18c}$$

$$p_k \le x_k \le q_k, \qquad k = 1, \ldots, n \tag{18d}$$

where $f(\underline{\boldsymbol{x}})$ is an objective function, $g_i(\underline{\boldsymbol{x}})$ are inequality constraints, $h_j(\underline{\boldsymbol{x}})$ are equality constraints, and $\underline{\boldsymbol{x}} = \{x_1, x_2, \ldots, x_n\}^T$ is a vector of design variables.

For the general optimization problem of Eqs. (18a–18d), a linearized problem may be constructed by approximating the nonlinear functions about a current solution point, $\underline{\boldsymbol{x}}_0 = \{x_{01}, x_{02}, \ldots, x_{0n}\}^T$, in a first-order Taylor-series expansion as follows:
maximize

$$f(\boldsymbol{x}) = f(\underline{\boldsymbol{x}}_0) + \nabla f(\underline{\boldsymbol{x}}_0)^T \delta\underline{\boldsymbol{x}} \tag{19a}$$

subjected to

$$g_i(\underline{\boldsymbol{x}}) = g_i(\underline{\boldsymbol{x}}_0) + \nabla g_i(\underline{\boldsymbol{x}}_0)^T \delta\underline{\boldsymbol{x}} \le 0 \tag{19b}$$

$$h_j(\underline{\boldsymbol{x}}) = h_j(\underline{\boldsymbol{x}}_0) + \nabla h_j(\underline{\boldsymbol{x}}_0)^T \delta\underline{\boldsymbol{x}} = 0 \tag{19c}$$

$$p_k \le x_k \le q_k \tag{19d}$$

where $i = 1, \ldots, r$; $j = r + 1, \ldots m$; $k = 1, \ldots, n$; $\delta\underline{\boldsymbol{x}} = \{x_1 - x_{01}, x_2 - x_{02}, \ldots, x_n - x_{0n}\}^T$.

It is clear that Eqs. (19a–19d) represent a linear programming problem where variables are contained in the vector $\delta\underline{\boldsymbol{x}}$. A solution for Eqs. (19a–19d) may be easily obtained by the simplex method.[24] After obtaining a solution of Eqs. (19a–19d), say $\underline{\boldsymbol{x}}_1$, we can linearize the original problem [Eqs. (18a–18d)] at $\underline{\boldsymbol{x}}_1$ and solve the new linear programming problem. The process is repeated until a precise solution is achieved. This approach is referred to as sequential linear programming.[17,18]

Although the procedure for a sequential linear programming is simple, difficulties may arise during the iterations. First, the optimum solution for the approximate linear problem may violate the constraint conditions of the original optimization problem. Second, in a nonlinear problem the true optimum solution may appear between two constraint intersections. A straightforward successive linearization may lead to an oscillation of the solution between the widely separated values. Difficulties in dealing with such a problem may be avoided by imposing a move limit on the linear approximation.[17,18] The concept of a move limit is that a set of box-like admissible constraints are placed in the range of $\delta\underline{\boldsymbol{x}}$ and it should gradually approach zero as the iterative process continues. It is known that computational economy and accuracy of the approximate solution may depend greatly on the choice of the move limit. In general, the choice of a suitable move limit depends on experience and also on the results of previous steps.

The algorithm of the sequential linear programming with selected move limits may be summarized as follows:

1) Linearize the nonlinear objective function and associated constraints with respect to an initial guess $\underline{\boldsymbol{x}}_0$.

2) Impose move limits in the form of $-\underline{\boldsymbol{S}} \leq (\underline{\boldsymbol{x}} - \underline{\boldsymbol{x}}_0) \leq \underline{\boldsymbol{R}}$, where $\underline{\boldsymbol{S}}$ and $\underline{\boldsymbol{R}}$ are properly chosen lower and upper bounds.

3) Solve the approximate linear programming problem to obtain an optimum solution $\underline{\boldsymbol{x}}_1$.

4) Repeat the procedures from 1 to 3 by redefining $\underline{\boldsymbol{x}}_1$ with $\underline{\boldsymbol{x}}_0$ until either the subsequent solutions do not change significantly, i.e., true convergence, or the move limit approaches zero, i.e., forced convergence. If the solution obtained is caused by forced convergence, the procedures from 1 to 4 should be repeated with another initial guess.

Convergence Study

Prior to the numerical analysis, convergence study of the shell element has been performed to analyze an isotropic square plate with four simply supported edges. The thickness of the plate is 0.001 m, and the length of one side of the plate is 0.1 m. The material properties are $E = 206$ GPa, $\nu = 0.3$, and $\rho = 20.29$ kg/m^3. The analytical solution for the fundamental frequency of the plate is $\omega = 60{,}188$ s^{-1}. In the numerical analysis, it is found that the use of 4×4 mesh (16 shell elements) to model the plate gives the same fundamental frequency as the exact solution. On the basis of this result and previous experience,[25,26] it is decided to use at least 36 elements (6×6 mesh) to model the laminated cylindrical panels having equal lengths in straight and curved edges. For panels with large aspect ratios or with cutouts, more elements are employed to model the entire structures.

Numerical Analysis

Laminated Cylindrical Panels with Various Curvatures and End Conditions

In this section, composite-laminated cylindrical panels with four types of end conditions (Fig. 2) are considered, which are four edges simply supported (denoted by SSSS), two curved edges simply supported and two straight edges fixed (denoted by SFSF), two curved edges fixed and two straight edges simply supported (denoted by FSFS), and four edges fixed (denoted by FFFF). In Fig. 2, ϕ is the circular angle of the curved edges, and x, y, and z are the axial direction, the tangent direction, and the normal direction of the panels, respectively. The lengths of the straight edge, a, and the curved edge, b, are all equal to 10 cm, and the circular angle ϕ varies between 5 and 150 deg. The thickness of each ply is 0.125 mm. The laminate layups of the plates are $[\pm\theta/90/0]_{ns}$. To study the influence of panel thickness on the results of optimization, $n = 2$ (16-ply thin panel) and 10 (80-ply thick panel) are selected for analysis. The lamina is composed of graphite/epoxy (Hercules AS/3501-6), and the material constitutive properties are taken from Crawley,[4] which are $E_{11} = 128$ GPa, $E_{22} = 11$ GPa, $\nu_{12} = 0.25$, $G_{12} = G_{13} = 4.48$ GPa, $G_{23} = 1.53$ GPa, $\rho = 1.5 \times 10^3$ kg/m^3. In the finite element analysis, no symmetry simplifications are made for those panels.

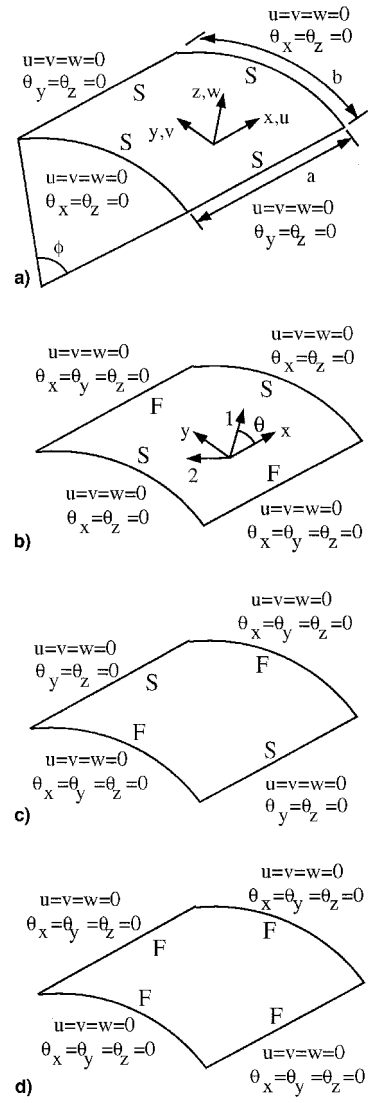

Fig. 2 Laminated curved panels with various end conditions: a) SSSS, b) SFSF, c) FSFS, and d) FFFF panels.

Based on the sequential linear programming method, in each iteration the current linearized optimization problem becomes

maximize:

$$\omega(\theta) = \omega(\theta_0) + (\theta - \theta_0) \left.\frac{\partial \omega}{\partial \theta}\right|_{\theta=\theta_0} \tag{20a}$$

subjected to:

$$0 \leq \theta \leq 90 \text{ deg} \tag{20b}$$

$$-r \times q \times 0.5^s \leq (\theta - \theta_0) \leq r \times q \times 0.5^s \tag{20c}$$

where ω is the fundamental frequency. The θ_o is a solution obtained in the previous iteration. The r and q in Eq. (20c) are the size and the reduction rate of the move limit. Based on past experience,[25,26] the values of r and q are selected to be 10 deg and $0.9^{(N-1)}$ in the present study, where N is a current iteration number. To control the oscillation of the solution, a parameter 0.5^s is introduced in the move limit, where s is the number of oscillations of the derivative $\partial\omega/\partial\theta$ that has taken place before the current iteration. The value of s increases by 1 if the sign of $\partial\omega/\partial\theta$ changes. Whenever oscillation of the solution occurs, the range of the move limit is reduced to half of its current value. This expedites the solution convergence rate very rapidly.

The $\partial\omega/\partial\theta$ term in Eq. (20a) may be approximated by using a forward finite difference method with the following form:

$$\frac{\partial\omega}{\partial\theta} = \frac{[\omega(\theta_o + \Delta\theta) - \omega(\theta_o)]}{\Delta\theta} \tag{21}$$

Hence, to determine the value of $\partial\omega/\partial\theta$ numerically, two finite element analyses to compute $\omega(\theta_o)$ and $\omega(\theta_o + \Delta\theta)$ are needed in each iteration. In this study, the value of $\Delta\theta$ is selected to be 1 deg in most iterations.

Figure 3 shows the optimal fiber angle θ and the associated optimal fundamental frequency ω with respect to the circular angle ϕ for thin $([\pm\theta/90/0]_{2s})$ laminated cylindrical panels. From Fig. 3a, we can see that when ϕ is less than 60 deg, the end conditions have a significant influence on optimal fiber angles of the panels. However, when ϕ is greater than 60 deg, the optimal fiber angles of these panels with different end conditions seem to be very close and vary around 60 deg. Figure 3b shows that ω increases with the increase of ϕ. Among these panels under the same geometric configuration, the FFFF panels have the highest optimal fundamental frequencies, and the SSSS panels have the lowest optimal fundamental frequencies. In addition, the optimal fundamental frequencies of SFSF panels are very close to those of FFFF panels, and the optimal fundamental frequencies of FSFS panels are very similar to those of SSSS panels. This indicates the panels at this geometric configuration are governed by the boundary conditions at the straight sides.

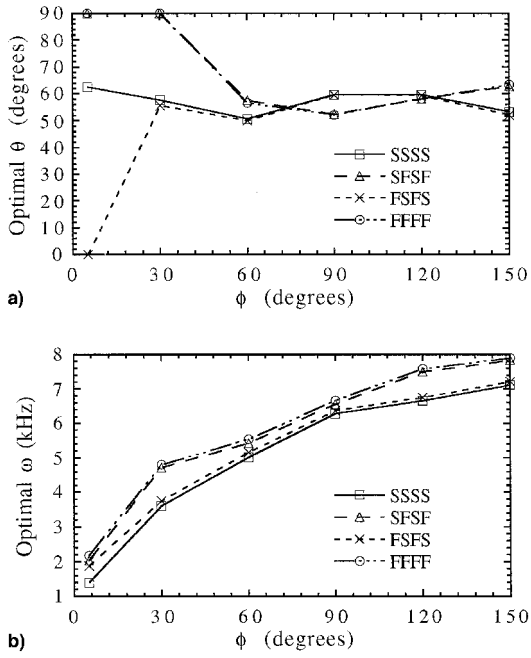

Fig. 3 Effect of end conditions and curvatures on a) optimal fiber angle and b) optimal fundamental frequency of thin $([\pm\theta/90/0]_{2s})$ laminated cylindrical panels (a/b = 1).

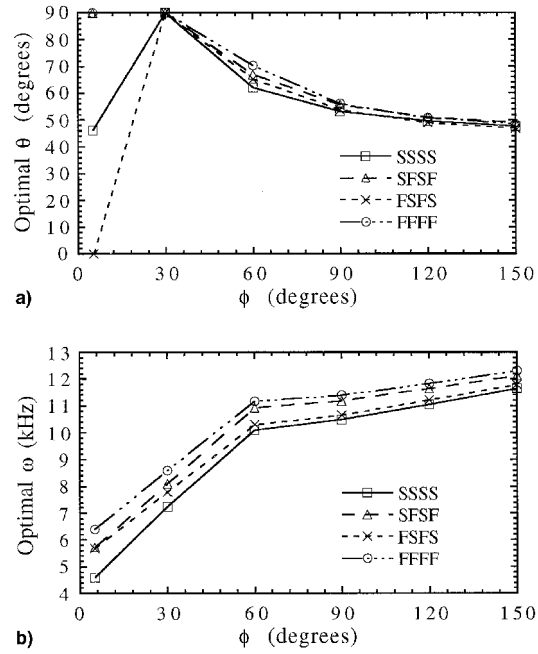

Fig. 4 Effect of end conditions and curvatures on a) optimal fiber angle and b) optimal fundamental frequency of thick $([\pm\theta/90/0]_{10s})$ laminated cylindrical panels (a/b = 1).

Figure 4 shows θ and ω with respect to ϕ for thick $([\pm\theta/90/0]_{10s})$ laminated cylindrical panels. Figure 4a shows that when ϕ is less than 30 deg, the end conditions have a significant influence on θ of the panels. However, when ϕ is greater than 30 deg, the optimal fiber angles of these panels with different end conditions seem to be very close and gradually decrease with the increase of ϕ. Comparing Fig. 4a with Fig. 3a, we can observe that thickness has a significant influence on the optimal fiber angles of the cylindrical panels. From Fig. 4b we can observe that these thick panels are also governed by the boundary conditions at the straight sides and ω increases with the increase of the panel curvature as thin panels.

Figure 5 shows the typical fundamental vibration modes for both thin and thick $([\pm\theta/90/0]_{2s}$ and $[\pm\theta/90/0]_{10s})$ panels with four fixed ends and under an optimal fiber orientation. We find that as panel curvatures increase, the vibration modes of these panels have more waves in the circumferential direction. Similar results are also obtained for panels with other end conditions.[27]

Laminated Cylindrical Panels with Various Aspect Ratios and End Conditions

In this section, laminated cylindrical panels with various aspect ratios a/b are analyzed. The length of the curved edge b is equal to 10 cm, and the length of the straight edge a varies between 2–30 cm (Fig. 2). The circular angle ϕ of these panels is set to 60 deg. Four types of end conditions, i.e., SSSS, SFSF, FSFS, and FFFF, described in a previous section, are considered. Again, the laminate layups, $[\pm\theta/90/0]_{2s}$ and $[\pm\theta/90/0]_{10s}$, are selected for analysis.

Figure 6 shows θ and ω with respect to the aspect ratio a/b for thin $([\pm\theta/90/0]_{2s})$ laminated cylindrical panels. From Fig. 6a, we can see that the results of optimization for these panels with different end conditions exhibit a similar trend. With an increase of the aspect ratio a/b, the optimal fiber angles all change from 0 to 90 deg. However, these transitional ranges in the aspect ratio for SSSS and FSFS panels are wider than those for SFSF and FFFF panels. The results in Fig. 6b show that as a/b increases, the optimal fundamental frequencies of these panels diminish to constant values. Generally, when the

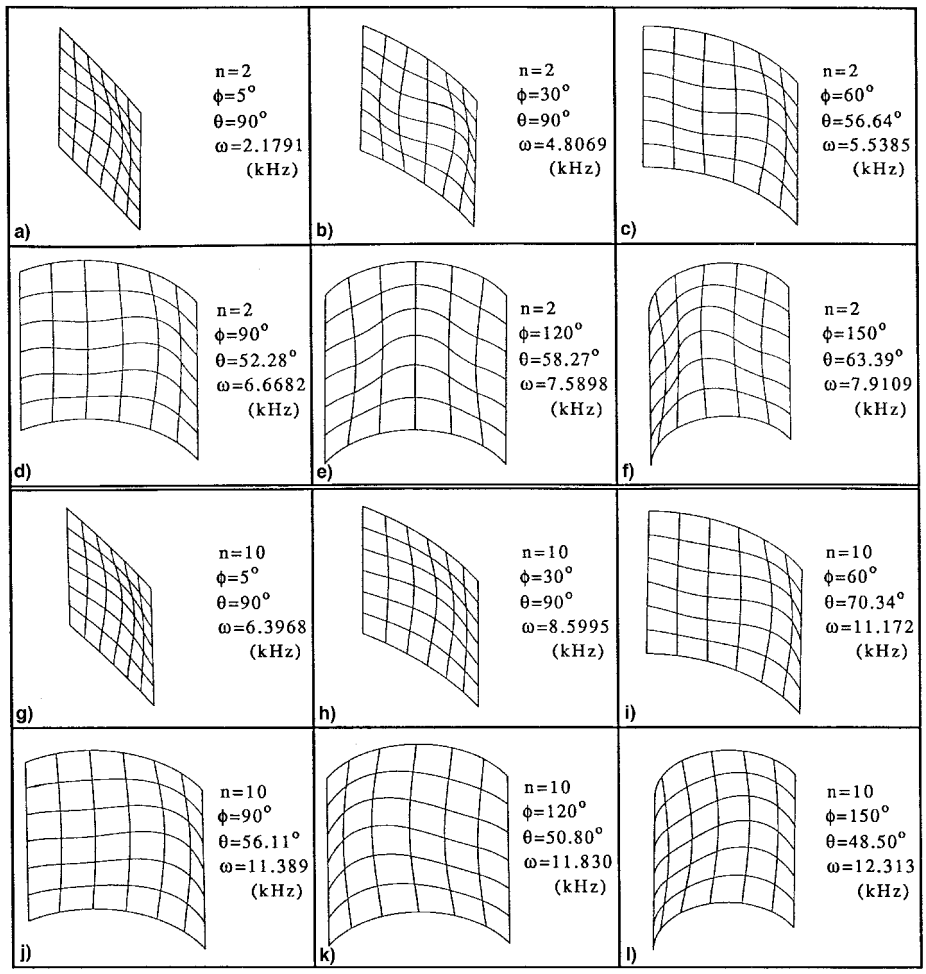

Fig. 5 Fundamental vibration mode of FFFF laminated cylindrical panels with $[\pm\theta/90/0]_{ns}$ layup and under optimal fiber angles (a/b = 1).

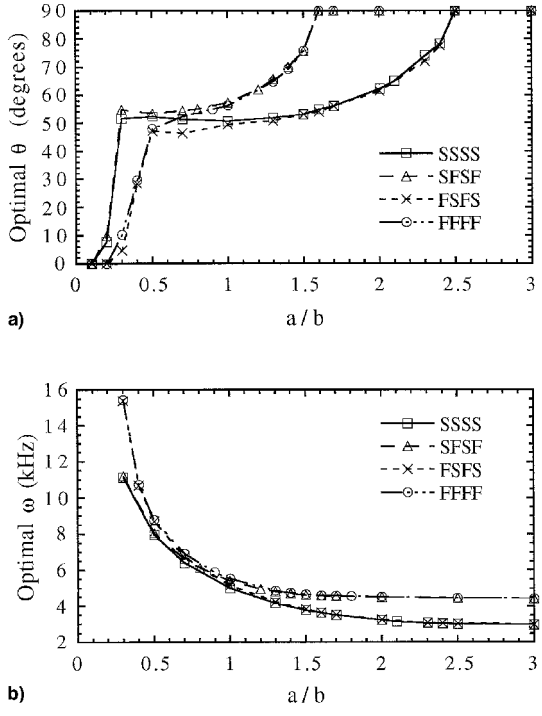

Fig. 6 Effect of end conditions and aspect ratios on a) optimal fiber angle and b) optimal fundamental frequency of thin ($[\pm\theta/90/0]_{2s}$) laminated cylindrical panels (ϕ = 60 deg).

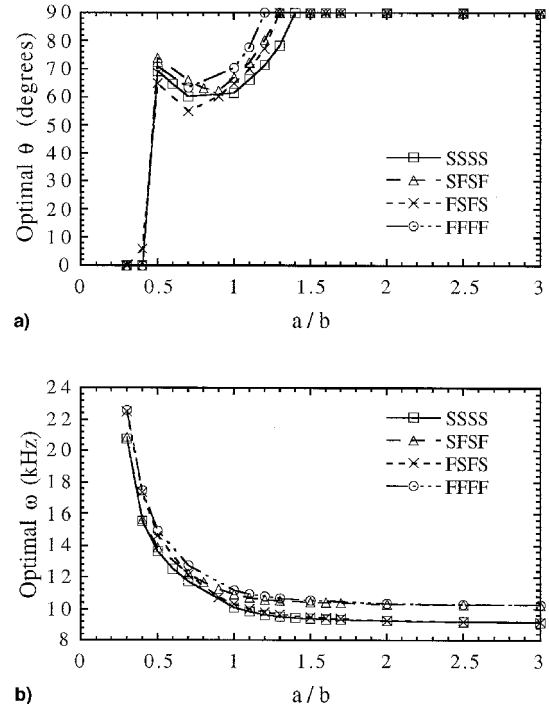

Fig. 7 Effect of end conditions and aspect ratios on a) optimal fiber angle and b) optimal fundamental frequency of thick ($[\pm\theta/90/0]_{10s}$) laminated cylindrical panels (ϕ = 60 deg).

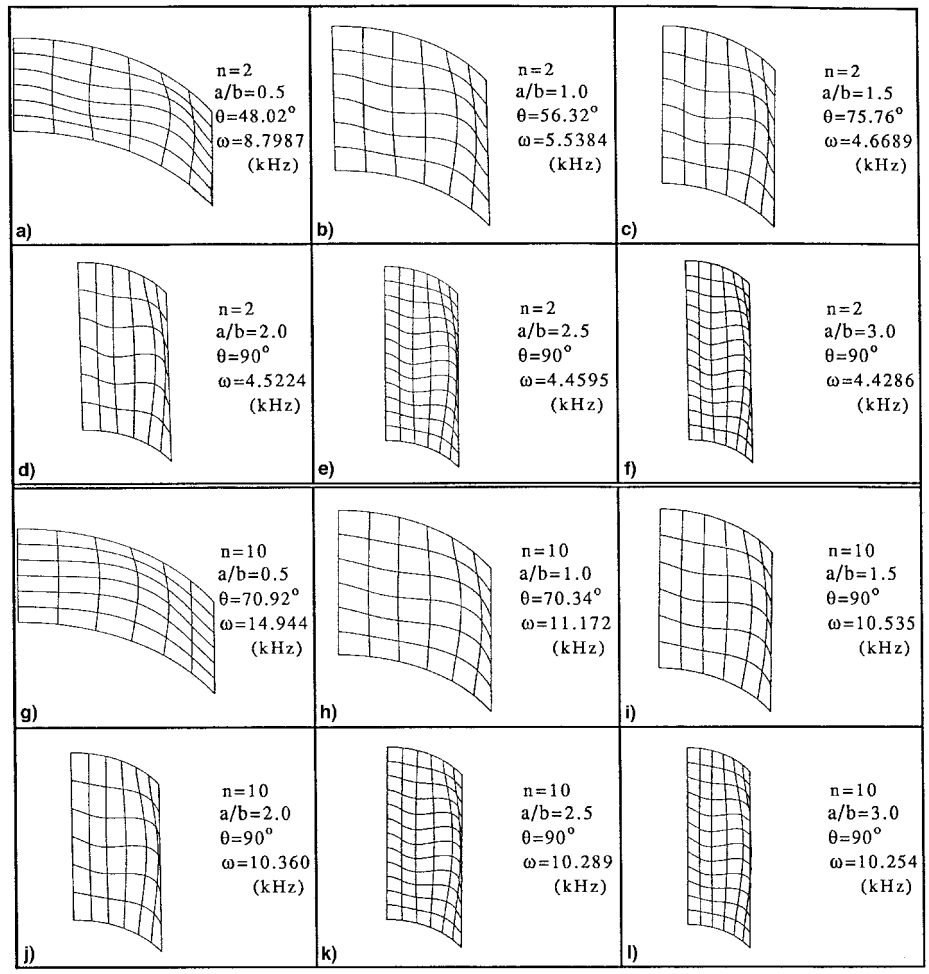

Fig. 8 Fundamental vibration mode of FFFF laminated cylindrical panels with $[\pm\theta/90/0]_{2s}$ layup and under optimal fiber angles (ϕ = 60 deg).

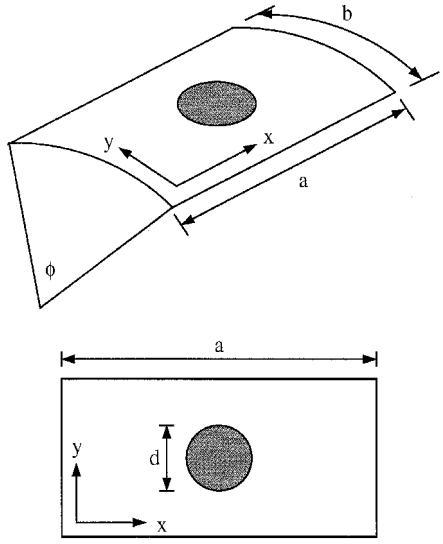

Fig. 9 Laminated curved panels with central circular cutout.

aspect ratio is small, e.g., $a/b < 0.5$, the results of optimization for SFSF panels are similar to those of SSSS panels, and the results of optimization for FSFS panels are similar to those of FFFF panels. However, when the aspect ratio is large, e.g., $a/b > 1$, the results of optimization for SFSF panels are similar to those of FFFF panels and the results of optimization for FSFS panels are similar to those of SSSS panels. This indicates

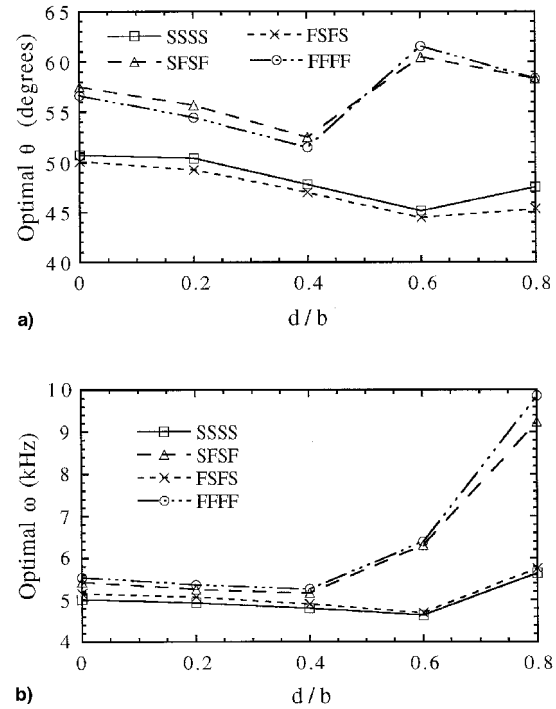

Fig. 10 Effect of end conditions and cutout sizes on a) optimal fiber angle and b) optimal fundamental frequency of thin ($[\pm\theta/90/0]_{2s}$) laminated cylindrical panels (a/b = 1, ϕ = 60 deg).

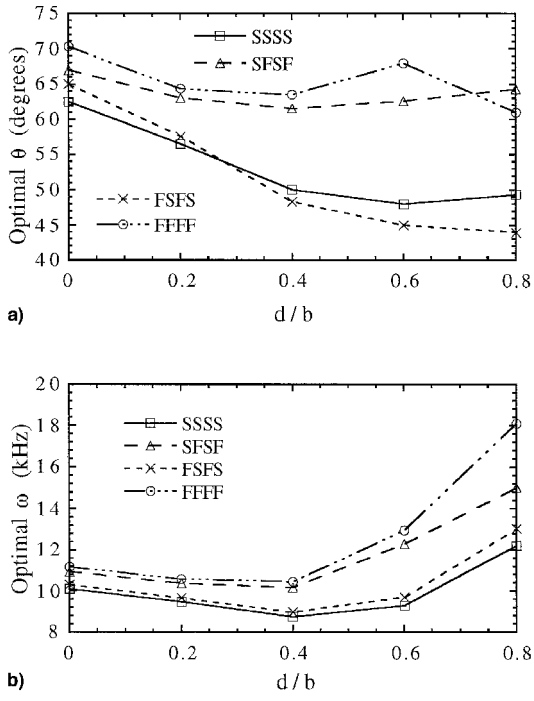

Fig. 11 Effect of end conditions and cutout sizes on a) optimal fiber angle and b) optimal fundamental frequency of thick ($[\pm\theta/90/0]_{10s}$) laminated cylindrical panels (a/b = 1, ϕ = 60 deg).

that the panels are governed by the boundary conditions at the curved sides for short panels and governed by the boundary conditions at the straight edges for long panels.

Figure 7 shows θ and ω with respect to the aspect ratio a/b for thick ($[\pm\theta/90/0]_{10s}$) laminated cylindrical panels. Figure 7a indicates again that with an increase of the aspect ratio, the optimal fiber angles of these panels all change from 0 to 90 deg. However, it seems that the influence of end conditions on the optimal fiber angles gradually disappears as the thicknesses of the panels are increased. Figure 7b shows a trend similar to Fig. 6b, except that the values of the optimal fundamental frequencies of thick panels are higher than those of thin panels. Typical fundamental vibration modes for both thin and thick ($[\pm\theta/90/0]_{2s}$ and $[\pm\theta/90/0]_{10s}$) panels with four fixed ends and under optimal fiber orientations are given in Fig. 8.

Laminated Cylindrical Panels with Various Central Circular Cutouts and End Conditions

In this section, laminated cylindrical panels with $a = b = 10$ cm, $\phi = 60$ deg are analyzed (Fig. 9). These panels contain central circular cutouts with diameter d, which varies between 2–8 cm. As before, four types of end conditions and two laminate layups, $[\pm\theta/90/0]_{2s}$ and $[\pm\theta/90/0]_{10s}$, are selected for analysis.

Figure 10 shows θ and ω with respect to the ratio d/b for thin ($[\pm\theta/90/0]_{2s}$) laminated cylindrical panels. From Fig. 10a, it can be seen that these panels are governed by the boundary conditions at the straight edges and the values of optimal fiber angles of SFSF and FFFF panels are greater than those of FSFS and SSSS panels. Figure 10b shows that when the cutout

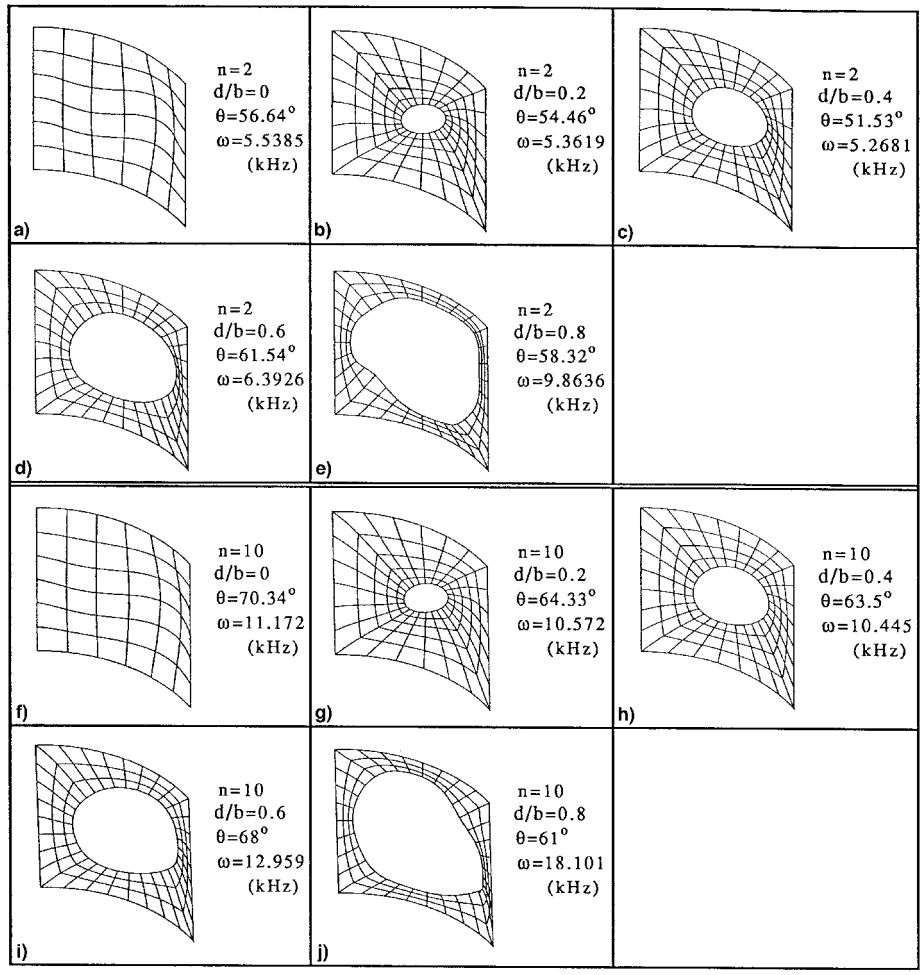

Fig. 12 Fundamental vibration mode of FFFF laminated cylindrical panels with $[\pm\theta/90/0]_{2s}$ layup, with circular cutouts and under optimal fiber angles (a/b = 1, ϕ = 60 deg).

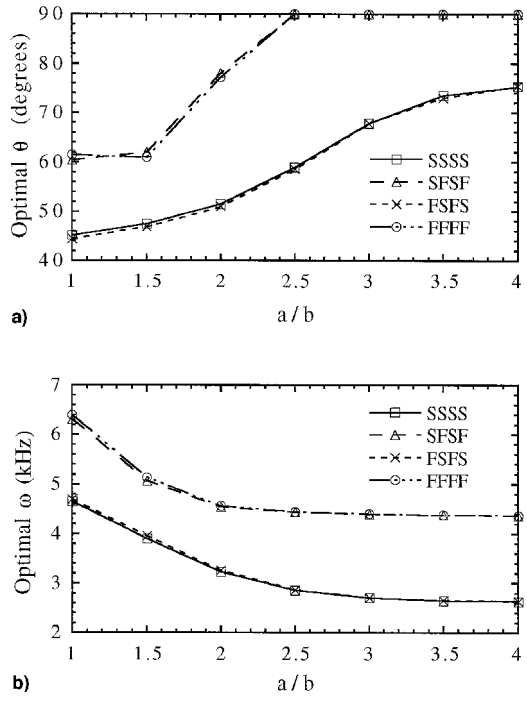

Fig. 13 Effect of end conditions and aspect ratios on a) optimal fiber angle and b) optimal fundamental frequency of thin ($[\pm\theta/90/0]_{2s}$) laminated cylindrical panels containing cutout (d/b = 0.6, ϕ = 60 deg).

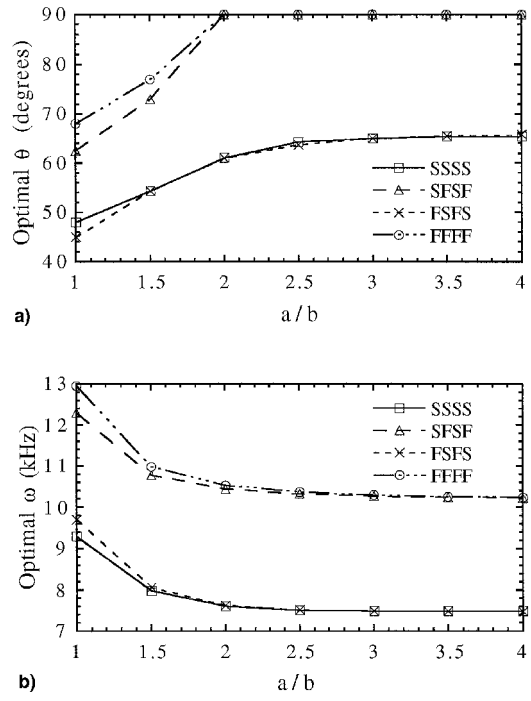

Fig. 14 Effect of end conditions and aspect ratios on a) optimal fiber angle and b) optimal fundamental frequency of thick ($[\pm\theta/90/0]_{10s}$) laminated cylindrical panels containing cutout (d/b = 0.6, ϕ = 60 deg).

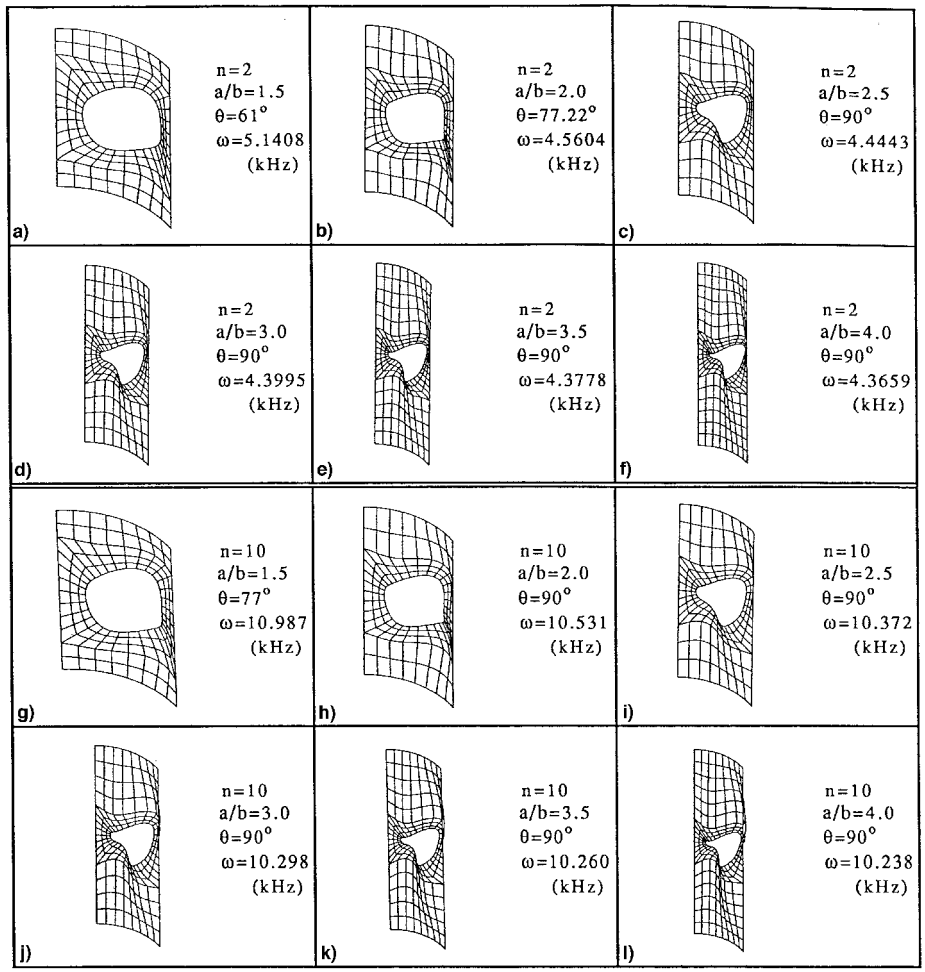

Fig. 15 Fundamental vibration mode of FFFF laminated cylindrical panels with $[\pm\theta/90/0]_{2s}$ layup, with circular cutouts and under optimal fiber angles (d/b = 0.6, ϕ = 60 deg).

sizes are small, the optimal fundamental frequencies decrease with the increase of the cutout sizes. However, when the cutout sizes are large, e.g., $d/b > 0.4$ for SFSF and FFFF panels, and $d/b > 0.6$ for FSFS and SSSS panels, the optimal fundamental frequencies increase with the increase of the cutout sizes. This is because a plate with a large cutout is more like four stubby cantilevered plates. As a consequence, one could expect frequencies to increase with d/b ratio.[6,9,26]

Figure 11 shows θ and ω with respect to the aspect ratio d/b for thick ($[\pm\theta/90/0]_{10s}$) laminated cylindrical panels. Figure 11a indicates that these thick panels are governed by the boundary conditions at the straight edges and the values of optimal fiber angles of SFSF and FFFF panels are greater than those of FSFS and SSSS panels. Figure 11b shows that the optimal fundamental frequencies decrease with the increase of the cutout sizes for small d/b ratios and increase with the increase of the cutout sizes for large d/b ratios.

Typical fundamental vibration modes for both thin and thick ($[\pm\theta/90/0]_{2s}$ and $[\pm\theta/90/0]_{10s}$) panels with four fixed ends and under optimal fiber orientations are given in Fig. 12. These modes show that when the cutout sizes are small, the fundamental vibration modes are global, i.e., vibration of entire panel. However, when the cutout sizes are large, the fundamental vibration modes are local, i.e., vibration of panel area near hole. Similar results are also obtained for panels with other end conditions.[27]

Laminated Cylindrical Panels Containing Central Circular Cutouts with Various Aspect Ratios and End Conditions

In this section, laminated cylindrical panels with $b = 10$ cm, $\phi = 60$ deg are analyzed (Fig. 9). The length of the straight edge a varies between 10–40 cm. These panels contain central circular cutouts with $d = 6$ cm. As before, four types of end conditions, SSSS, SFSF, FSFS, FFFF, and two laminate layups, $[\pm\theta/90/0]_{2s}$ and $[\pm\theta/90/0]_{10s}$, are selected for analysis.

Figures 13 and 14 show θ and ω with respect to the aspect ratio a/b for both thin and thick ($[\pm\theta/90/0]_{2s}$ and $[\pm\theta/90/0]_{10s}$) laminated cylindrical panels. Figures 13a and 14a show that, generally, the optimal fiber angles increase with an increase of panel aspect ratio. For SFSF and FFFF panels, the optimal fiber angles are fixed to 90 deg when a/b ratios are large. However, it seems that the optimal fiber angles for FSFS and SSSS panels do not reach 90 deg, even for large a/b ratios. Comparing Figs. 13a and 14a with Figs. 6a and 7a, we can see that the cutouts have a significant influence on the optimal fiber angles of curved panels. From Figs. 13b and 14b we can see that as a/b increases, the optimal fundamental frequencies of these panels gradually decrease and diminish to constant values.

Typical fundamental vibration modes for both thin and thick ($[\pm\theta/90/0]_{2s}$ and $[\pm\theta/90/0]_{10s}$) panels with four fixed ends and under optimal fiber orientations are given in Fig. 15. These modes show that when the panel aspect ratios are small, the fundamental vibration modes are global. However, when the panel aspect ratios are large, the fundamental vibration modes are local to the holes. Similar results are also obtained for panels with other end conditions.[27]

Conclusions

In the process of sequential linear programming, most optimal results are obtained within 12 iterations, and the results are all verified by choosing different initial guesses. Hence, the sequential linear programming is efficient and stable to solve nonlinear optimization problems.

Generally, thicknesses, end conditions, curvatures, aspect ratios, and circular cutouts have a significant influence on the optimal fiber angles and optimal fundamental frequencies of $[\pm\theta/90/0]_{ns}$ laminated curved panels. To be more specific, the following conclusions may be drawn:

1) The results of optimization for short laminated curved panels are similar when they have the same boundary conditions at the curved edges. However, the results of optimization for long panels are similar when they have the same boundary conditions at the straight sides. For curved panels without cutouts, the influence of end conditions on the optimal fiber angles gradually disappears as the thicknesses of the panels are increased.

2) The optimal fundamental frequency of the curved panel increases with the increasing of panel curvature. In addition, the vibration mode of the panel would have more waves in the circumferential direction if the panel curvature was increased.

3) When the panel aspect ratio becomes large, the optimal fiber angles for laminated curved panels with and without cutouts gradually approach 90 deg, except those panels with cutouts and with FSFS and SSSS ends. Nevertheless, the optimal fundamental frequencies of the panels will be reduced and diminish to constant values as the aspect ratio becomes large.

4) The introduction of cutouts may increase the optimal fundamental frequencies of laminated curved panels, and the optimal fundamental frequencies of curved panels may increase with the increase of the sizes of cutouts. When the cutout sizes are small, the fundamental vibration modes are global. However, when the cutout sizes are large, the fundamental vibration modes are local to the holes.

5) For laminated curved panels with fixed cutout size, when the panel aspect ratios are small, the fundamental vibration modes may be global. However, when the panel aspect ratios are large, the fundamental vibration modes may be local to the holes.

Acknowledgment

This work was financially supported by the National Science Council of the Republic of China under Grant NSC 85-2211-E006-006.

References

[1]Leissa, A. W., "Recent Research in Plate Vibrations. 1973–1976: Complicating Effects," *The Shock and Vibration Digest*, Vol. 10, No. 12, 1978, pp. 21–35.

[2]Leissa, A. W., "Plate Vibrations Research, 1976–1980: Complicating Effects," *The Shock and Vibration Digest,* Vol. 13, No. 10, 1981, pp. 19–36.

[3]Leissa, A. W., "Recent Studies in Plate Vibrations: 1981–85, Part II. Complicating Effects," *The Shock and Vibration Digest,* Vol. 19, No. 3, 1987, pp. 10–24.

[4]Crawley, E. F., "The Natural Modes of Graphite/Epoxy Cantilever Plates and Shells," *Journal of Composite Materials,* Vol. 13, July 1979, pp. 195–205.

[5]Sharma, C. B., and Darvizeh, M., "Free Vibration of Specially Orthotropic, Multilayered, Thin Cylindrical Shells with Various End Conditions," *Composite Structures,* Vol. 7, No. 2, 1987, pp. 123–138.

[6]Lee, H. P., Lim, S. P., and Chow, S. T., "Free Vibration of Composite Rectangular Plates with Rectangular Cutouts," *Composite Structures,* Vol. 8, No. 1, 1987, pp. 63–81.

[7]Chandrashekhara, K., "Free Vibration of Anisotropic Laminated Doubly Curved Shells," *Computers and Structures,* Vol. 33, No. 2, 1989, pp. 435–440.

[8]Qatu, M. S., and Leissa, A. W., "Natural Frequencies for Cantilevered Doubly-Curved Laminated Composite Shallow Shells," *Composite Structures*, Vol. 17, No. 3, 1991, pp. 227–255.

[9]Ramakrishna, S., Rao, K. M., and Rao, N. S., "Free Vibration Analysis of Laminates with Circular Cutout by Hybrid-Stress Finite Element," *Composite Structures,* Vol. 21, No. 3, 1992, pp. 177–185.

[10]Raouf, R. A., "Tailoring the Dynamic Characteristics of Composite Panels Using Fiber Orientation," *Composite Structures*, Vol. 29, No. 3, 1994, pp. 259–267.

[11]Liu, H. W., and Huang, C. C., "Free Vibrations of Thick Cantilever Laminated Plates with Step-Change of Thickness," *Journal of Sound and Vibration*, Vol. 169, No. 5, 1994, pp. 601–618.

[12]Chun, L., and Lam, K. Y., "Dynamic Analysis of Clamped Laminated Curved Panels," *Composite Structures*, Vol. 30, No. 4, 1995, pp. 389–398.

[13]Bert, C. W., "Optimal Design of a Composite-Material Plate to Maximize Its Fundamental Frequency," *Journal of Sound and Vibra-*

tion, Vol. 50, No. 2, 1977, pp. 229–237.

[14]Abrate, S., "Optimal Design of Laminated Plates and Shells," *Composite Structures*, Vol. 29, No. 3, 1994, pp. 269–286.

[15]Bert, C. W., "Literature Review—Research on Dynamic Behavior of Composite and Sandwich Plates—V: Part II," *The Shock and Vibration Digest*, Vol. 23, No. 7, 1991, pp. 9–21.

[16]Schmit, L. A., "Structural Synthesis—Its Genesis and Development," *AIAA Journal*, Vol. 19, No. 10, 1981, pp. 1249–1263.

[17]Zienkiewicz, O. C., and Champbell, J. S., "Shape Optimization and Sequential Linear Programming," *Optimum Structural Design, Theory and Applications*, edited by R. H. Gallagher and O. C. Zienkiewicz, Wiley, New York, 1973, pp. 109–126.

[18]Vanderplaats, G. N., *Numerical Optimization Techniques for Engineering Design with Applications*, McGraw–Hill, New York, 1984, Chap. 6.

[19]*ABAQUS User, Theory and Verification Manuals*, Version 5.4, Hibbitt, Karlsson & Sorensen, Inc., Providence, RI, 1995.

[20]Irons, B. M., "The Semi-Loof Shell Element," *Finite Elements for Thin Shells and Curved Members,* edited by D. G. Ashwell and R. H. Gallagher, Wiley, London, 1976, pp. 197–222.

[21]Whitney, J. M., "Shear Correction Factors for Orthotropic Laminates Under Static Load," *Journal of Applied Mechanics,* Vol. 40, No. 1, 1973, pp. 302–304.

[22]Cook, R. D., Malkus, D. S., and Plesha, M. E., *Concepts and Applications of Finite Element Analysis*, 3rd ed., Wiley, New York, 1989, Chap. 13.

[23]Bathe, K. J., and Wilson, E. L., "Large Eigenvalue Problems in Dynamic Analysis," *Journal of Engineering Mechanics Division,* Vol. 98, 1972, pp. 1471–1485.

[24]Kolman, B., and Beck, R. E., *Elementary Linear Programming with Applications*, Academic, Orlando, FL, 1980.

[25]Hu, H.-T., and Wang, S. S., "Optimization for Buckling Resistance of Fiber-Composite Laminate Shells With and Without Cutouts," *Composite Structures,* Vol. 22, No. 1, 1992, pp. 3–13.

[26]Hu, H.-T., and Ho, M.-H., "Influence of Geometry and End Conditions on Optimal Fundamental Natural Frequencies of Symmetrically Laminated Plates," *Journal of Reinforced Plastics and Composites*, Vol. 15, No. 9, 1996, pp. 877–893.

[27]Juang, C.-D., "Influence of Geometry and End Conditions on Optimal Fundamental Frequencies and Associated Optimal Fiber Angles of Symmetrically Laminated Curved Panels," M.S. Thesis, Dept. of Civil Engineering, National Cheng Kung Univ., Tainan, ROC, 1995.